The Ultra-High-Resolution Facility at the Anglo−Australian Telescope

F. Diego,[1] A. C. Fish,[1] M. J. Barlow,[1] I. A. Crawford,[1] J. Spyromilio,[2]
M. Dryburgh,[1] D. Brooks,[1] I. D. Howarth[1] and D. D. Walker[1]

[1]*Department of Physics and Astronomy, University College London, Gower Street, London WC1E 6BT*
[2]*Anglo−Australian Observatory, PO Box 296, Epping, New South Wales 2121, Australia*

ABSTRACT

The Ultra-High-Resolution Facility (UHRF) has been commissioned at the coudé focus of the Anglo−Australian Telescope (AAT), and provides a resolving power of $R \approx 10^6$. This is the highest spectral resolution ever obtained by an optical astronomical spectrograph, and is intended mainly for astrophysical studies of cool interstellar clouds. This paper describes the development of this ambitious project, which includes diffraction-limited optical components, very tight specification for the optical configuration, and a new type of image slicer which allows ultra-high-resolution work towards faint stars. Astrophysical results from the first observing runs are presented to demonstrate the performance in terms of both resolution and throughput.

Key words: line: profiles − instrumentation: spectrographs − ISM: atoms − ISM: clouds.

1 INTRODUCTION

The study of the cool interstellar medium requires ultra-high spectral resolution techniques. Existing spectrographs used for this work (with maximum resolving powers given in parentheses) include the coudé instruments on the McDonald Observatory 2.7-m telescope ($R = 600\,000$, Tull 1972; Lambert, Sheffer & Crane 1990); the Mt Stromlo Observatory 1.9-m telescope ($R = 300\,000$, Butcher 1971; Crawford, Rees & Diego 1987); the Kitt Peak National Observatory 0.9-m coudé feed telescope ($R = 200\,000$, e.g. Meyer, Hawkins & Wright 1993), and the European Southern Observatory's 3.6- and 1.4-m coudé auxiliary telescopes ($R = 100\,000$, Enard 1982). The most extensive published set of high-resolution interstellar line observations are due to Hobbs (1969, and many subsequent papers), who used a triple-etalon Fabry−Perot interferometer to achieve resolving powers of about 150 000.

The astrophysical importance of even higher resolutions was stressed by Barlow (1984), who suggested the construction of a very long camera for the UCL Echelle Spectrograph (UCLES), then being built under a contract for the Anglo−Australian Observatory (AAO). [For UCLES, see Walker & Diego (1985), Hirst et al. (1986), Walker et al. (1986), Diego (1988a, b), Fish (1988) and Diego et al. (1990).] With such a camera it would be possible to obtain resolutions approaching the theoretical limit given by $R = n \times m$ (where n is the total number of grooves in the grating and m is the order of interference), or $R \sim 1.25 \times 10^6$

in the region of the Na I D lines. Although lack of AAO funds prevented this suggestion being taken up immediately, the opportunity presented by the bright supernova SN 1987A led Peter Gillingham of the AAO to construct a temporary coudé spectrograph, combining a novel Littrow lens design with one of the large echelle gratings eventually destined for UCLES (Gillingham 1988). The focal length of this spectrograph enabled the 408-mm long, 79 g mm^{-1} echelle to deliver a resolving power of about 820 000 in the region of the Na I D lines (Gillingham 1988; Pettini 1988).

The success of this experiment led to a renewal of efforts to provide a permanent facility at the AAT for ultra-high-resolution spectrography. An SERC Grant, which commenced in 1989, was obtained to develop what has become the Ultra-High-Resolution Facility (UHRF), and further resources allocated by the AAO have made it available as a common-user instrument. The design, construction and commissioning of UHRF were performed at the Optical Science Laboratory (OSL) of the Department of Physics and Astronomy of University College London.

UHRF incorporates Gillingham's basic design concept, with the addition of grating cross-dispersion and a general layout that fits within the UCLES environment, sharing most of the slit-area facilities (such as the calibration unit and acquisition and guiding) and the space in the east coudé room of the AAT.

It is intended that both UCLES and UHRF will share the same control software package and have similar user interfaces. The low-level control of both instruments will be

performed by a single microcomputer system (68000-based). High-level control and the user interface will be operated from the ADAM environment (STARLINK Project, UK).

In addition to its prime resolving power mode of one million, designed for interstellar absorption-line spectrography, the UHRF has lower resolution modes of (nominally) 3×10^5 and 6×10^5, suitable for investigating a range of specialized topics in stellar astrophysics.

A major innovation is the Confocal Image Slicer (Diego 1993), which increases by an order of magnitude the throughput of an ordinary narrow slit.

On-telescope commissioning tests have already produced scientific results (Barlow et al. 1995; Crawford et al. 1994a,b). These show that the UHRF meets its design specifications. To our knowledge, the UHRF is the highest resolution optical astronomical spectrograph ever built.

2 ASTROPHYSICAL CONSIDERATIONS

The unprecedented resolving power of one million was specified to tackle the following problems in interstellar medium research.

(1) The resolution of the thermally broadened line profiles of heavy atoms in a gas at a temperature of about 100 K (0.4 km s^{-1} FWHM for Na atoms, for example) would provide (for the first time at optical wavelengths) direct measurements of diffuse cloud temperatures. Moreover, by measuring the velocity dispersions of lines due to atoms with widely different masses, it would also be possible to determine both the kinetic temperature and the magnitude of any turbulent velocity fields that may be present within diffuse interstellar clouds.

(2) In addition, it is expected that the UHRF will make a significant contribution to the elucidation of the role of shocks in the interstellar medium. Shocks are often invoked, both in the context of grain-destruction mechanisms (e.g. Barlow & Silk 1977), and in the driving of endothermic chemical reactions (especially that required to produce interstellar CH$^+$; e.g. Elitzur & Watson 1978). The various shock models make detailed predictions concerning the profiles of spectral lines formed within them, but existing spectrographs have been unable to resolve this structure. In the particular case of CH$^+$, temperatures of about 3000 K are required (corresponding to shock velocities of about 10 km s^{-1}). This would result in a CH$^+$ velocity dispersion of 1.9 km s^{-1}, easily resolvable with the UHRF.

(3) Detection of weak interstellar lines: the factor of 10 increase in resolving power conferred by the UHRF will, for a given S/N ratio, reduce the minimum detectable equivalent width by the same factor. (Observations during the commissioning phase have already demonstrated the instrument's ability to measure equivalent widths as low as 0.2 mÅ routinely.)

(4) Very accurate measurements of radial velocities (to better than 0.1 km s^{-1}), and the unambiguous determination of the number of discrete absorption components present towards a given star, will be possible.

3 DESIGN PHILOSOPHY

The design of a facility able to meet the requirements described above was based on a grating spectrograph because of its clean instrumental profile, and the main specification was to sample it with four 10-μm pixels of the Image Photon Counting System (IPCS), equivalent to two 19-μm Thomson CCD pixels. The projection of a millionth of a wavelength on 40 μm implied a dispersion of ~1 Å cm^{-1}, which demanded the largest echelle grating commercially available, a camera about 10 m long and an entrance slit only 30 or 40 μm wide (typically 0.05 arcsec at the coudé focus of the AAT).

This approach was a severe challenge to the design, with the following technical requirements:

(i) near diffraction-limited optical performance;

(ii) spectral coverage from 3000 to 11 000 Å;

(iii) ability to scan the entire spectrum along and across the echelle orders with high accuracy, stability and repeatability;

(iv) wide separation between echelle orders required to accommodate the long slit produced by some kind of image slicer (which is essential to improve the very low transmission of a single extremely narrow slit), and

(v) anamorphic optics required to minimize the detector area occupied by the wide spectrum produced by the long slit. (Work is continuing on this aspect of the design; see Section 7.3.)

In addition, the optical and mechanical layouts were restricted by the location of UCLES components in the coudé room.

The original concept for UHRF involved a fully reflective system with a long-focus camera, interchangeable with the current 700-mm camera of UCLES and using grating cross-dispersion to (a) preserve near diffraction-limited performance, and (b) provide wider separation between the echelle orders (neither of which could be provided by the UCLES prisms). In the event, a more efficient approach (Section 4) was adopted, following the success of the spectrograph built by Gillingham (1988).

As with UCLES, the philosophy was to create an instrument with a friendly user interface, in order to keep the observer isolated from calculations of grating angles and positions (although this aspect of the control system has not yet been fully implemented; see Section 6.1).

4 OPTICAL LAYOUT

Fig. 1 is a simplified layout of UHRF: light coming from the 5th coudé mirror of the AAT (A) is directed to the aperture (B) of the Confocal Image Slicer (CIS, see Section 4.1), which produces a long and narrow optical slit. The field lens (C) works in combination with the beam-expanding lens (D) in order to overfill the echelle grating and to ensure that all the light from the slicer reaches it. A couple of interchangeable wheels (E) allow the use of special filters to isolate echelle orders or to suppress unwanted spectral regions which may cause stray light. The accurate shutter (F) is driven by the routines that control the detector to limit the exposure time. The collimator-echelle unit has a large aspheric collimating lens (G) mounted in double pass just in front of the echelle grating (H). The diffracted beam is directed to the cross-disperser unit, where it is collimated again by a diverging lens (I) before being reflected by one of the cross-disperser gratings installed in a rotating turret (J).
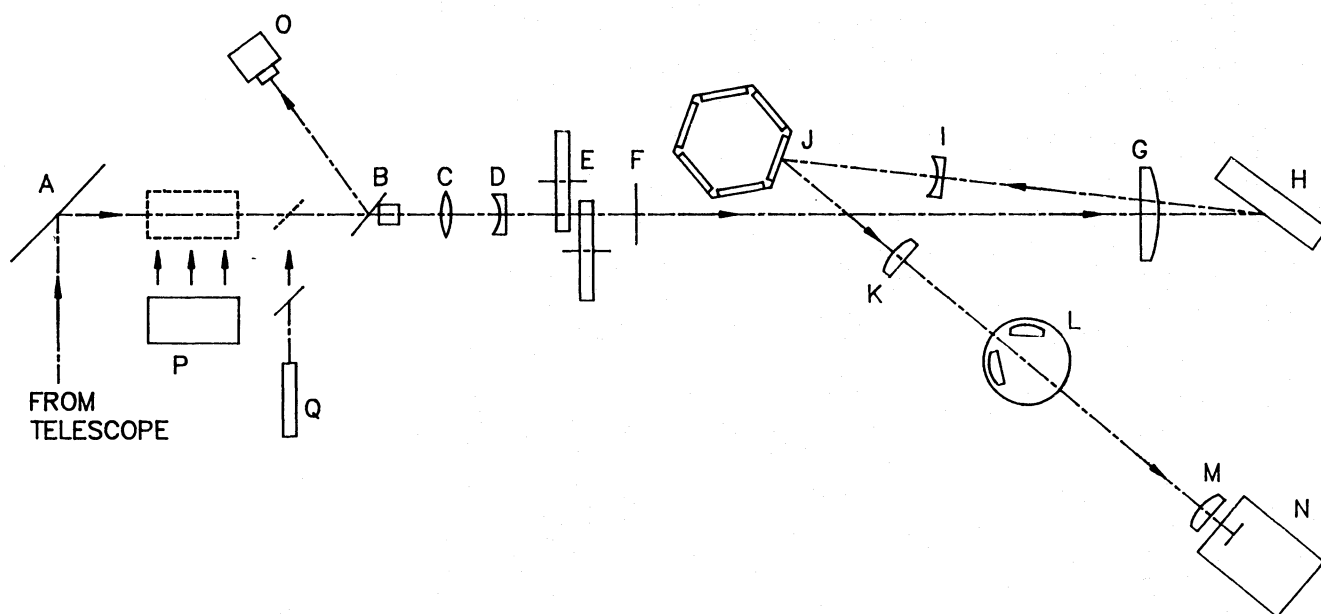
Figure 1. The UHRF optical layout (not to scale). The optical components are identified in the text (Section 4).

Finally, another aspheric lens (K) images the spectrum on the detector (N), just after a small and powerful cylindrical lens (M) collapses the projected length of the slit (but see Section 7.3). A motorized turret mechanism (L) can be used to interpose additional converging lenses, which reduce the total focal length to provide wider spectral coverages at lower resolutions.

Acquisition and guiding are done by an intensified CCD camera (O) which picks up the reflection from the tilted dekker plate of the CIS. A Th-Ar lamp (P) is placed directly in front of the CIS aperture for wavelength calibration purposes.

A frequency-stabilized He-Ne laser (Q) has been installed in one of the available ports of the UCLES calibration lamp unit. This provides an unresolved line at 6328.160 Å, which is used to evaluate and monitor the UHRF instrumental profile.

Fig. 2 (opposite p. 326) shows the instrument as installed in the east coudé room at the AAT. Both UCLES and UHRF are mounted on a massive steel frame, which floats on air pads to isolate the instruments from vibrations in the building. This feature is crucial to achieve ultra-high resolution.

4.1 Image-slicing system

The 35-μm entrance slit required for the UHRF projects to only 0.05 arcsec on the sky, which means a rejection of more than 97 per cent of the energy contained in a typical seeing disc of 1.5-arcsec FWHM. This prompted us to investigate in detail the possibility of image slicing. There are two kinds of image slicers currently in use: the Richardson (based on superimposing multiple reflections from concave mirrors, Richardson, Fletcher & Grundman 1984) and the Bowen-Walraven (based on multiple total internal reflections inside a thin parallel plate, Hunten 1974 and Simmons, Drake & Hepburn 1982).

In principle, the Bowen-Walraven slicer is more efficient and easier to implement, but it has the disadvantage of producing a 'slit' which is tilted along the optical axis, as the slicing takes place along the hypotenuse of a 45° prism. Consequently, only a short length of the slit within focus tolerance can be used, and the full potential of the device is wasted.

In view of this, it was decided to carry out some experiments based on the Bowen-Walraven design, and a method to generate an optical slit that is in focus over its entire length was developed. We call this device a Confocal Image Slicer (CIS, patent pending), and a detailed description has been published elsewhere (Diego 1993).

A CIS prototype was produced and tested during the first commissioning period of UHRF in 1992 July. This version (designated CIS-17) slices 17 times an area of 1 arcsec^2 at the core of the seeing disc, producing a slit 9 mm long and 40 μm wide on the detector. Later, a more ambitious version was developed and left permanently installed on UHRF after the second commissioning run in 1993 January. This is the CIS-35, which slices 35 times an area of 1.0×1.5 arcsec^2, producing a slit 20 mm long and 30 μm wide. An example of the output of the CIS-35 (masked down to 14 slices – see Section 7.3) is shown in Fig. 3 (opposite p. 326).

The slicer system also includes a converging field lens and a diverging beam-expanding lens. The former is mounted in the slicer housing, and the latter is mounted in one of the available slots in the focal modifier lens wheel of UCLES (see Fig. 1). Both have been calculated to expand the f/37.5 coudé beam to overfill the echelle grating by 25 per cent (Diego & Walker 1985). This means that the optical slit can be 25 per cent wider, which is very useful to facilitate the optical production of the CIS, and also to avoid excessive losses due to diffraction at a very narrow slit (Gillingham 1988). The set of lenses has also been calculated to superimpose all the slices on the echelle grating.

During the early stages of commissioning, a strong cylindrical lens was placed near the focal plane. Its function was to collapse the long image of the slit in order to reduce the width of the spectrum projected on the detector, thus

minimizing problems created by an excessive number of cosmic ray events, read-out noise and dark current contributions, all of them associated with CCD characteristics and proportional to its area. Behaving as a parallel plate in the spectral direction, the lens left the spectral resolution unaffected. However, it was found that use of this lens makes it impossible to sample directly the interorder light, which is needed in order to evaluate the background levels. We discuss this problem further in Section 7.3.

It is important to note that, although the UCLES slit can be used with the UHRF, it was not designed to provide reliable values of its width below 100 μm, so a manually adjusted slit can be placed in the CIS-35 position for calibration and engineering tests. This slit is also available to observers for special applications.

4.2 Echelle-collimator unit

This unit is the heart of the UHRF (Fig. 4, opposite p. 326). A large (300-mm diameter) fused-silica single lens is used as collimator just in front of a 204×408 mm^2 echelle grating ruled at 31.6 g mm^{-1} and blazed at a measured angle of 64°95 by Milton Roy Co., New York. The lens was polished and aspherized at OSL. The beam separation at the echelle grating is only 2°, and the diffracted beam is made convergent by passing again through the lens. Both components are installed in a sliding box, the position of which along the optical axis is adjusted very accurately as a function of wavelength (Fig. 5). In order to collimate beams from 3000 to 11 000 Å, the displacement needs to be as long as 450 mm, and the requested position is obtained within 50 μm by using coarse and fine linear actuators, with an absolute linear encoder measuring the real movement of the unit (this encoder is a Linear Variable Displacement Transducer, LVDT).

Following the same principle used for UCLES (Diego et al. 1990), the echelle grating pivots on knife-edges to allow scanning along the echelle orders (Fig. 6). A tangent arm mechanism is operated by a small linear actuator, and a linear encoder (another LVDT) measures the tilt angle with
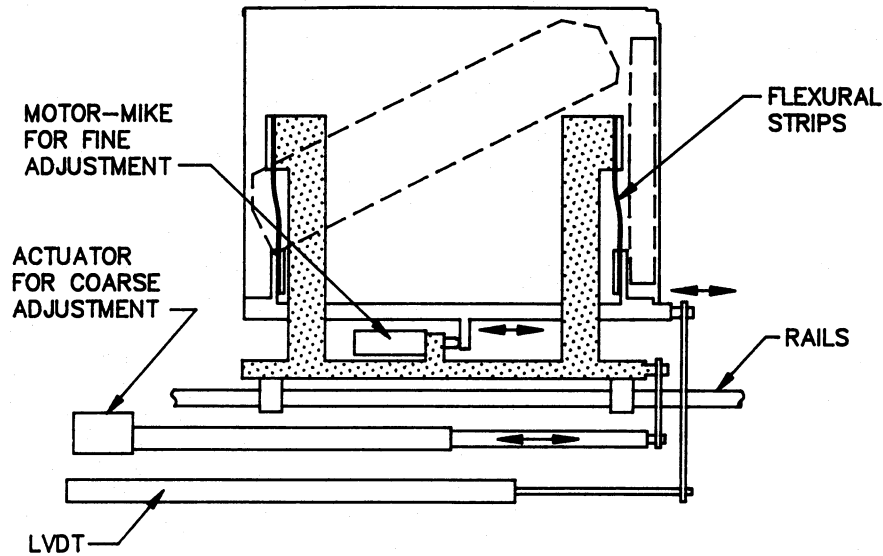

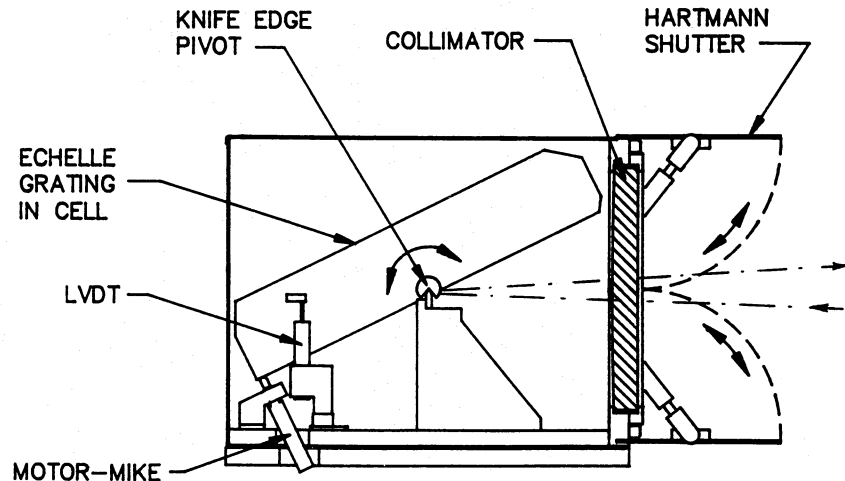**Figure 5.** The focusing mechanism of the echelle-collimator unit.

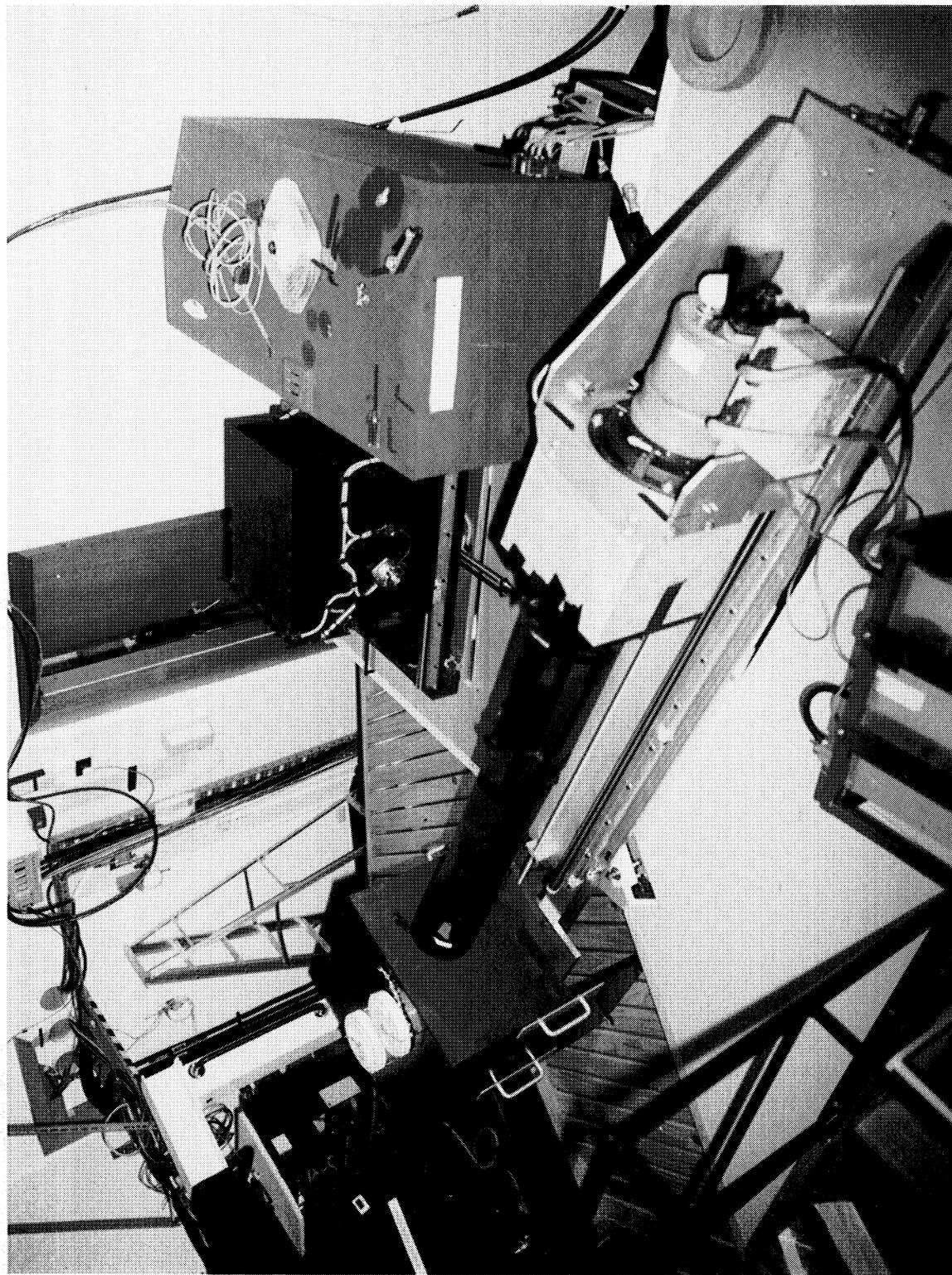**Figure 6.** Echelle tilt mechanism.

Figure 2. UCLES and UHRF components in the AAT coudé room. The UHRF echelle-collimator unit is the black box above the centre of the picture. To its right is the UCLES collimator unit. The rail in the foreground permits the detector to be repositioned for the different resolution modes. The box to the left of centre contains the focal reducer lenses. A cardboard tube was used as a baffle between this box and the detector carriage on the right, which contains a metal baffle, a fast shutter and the CCD cryostat. On the extreme left is the unit containing the cross-disperser turret, secondary collimator and imaging lens. Refer to Figs 1 and 9.
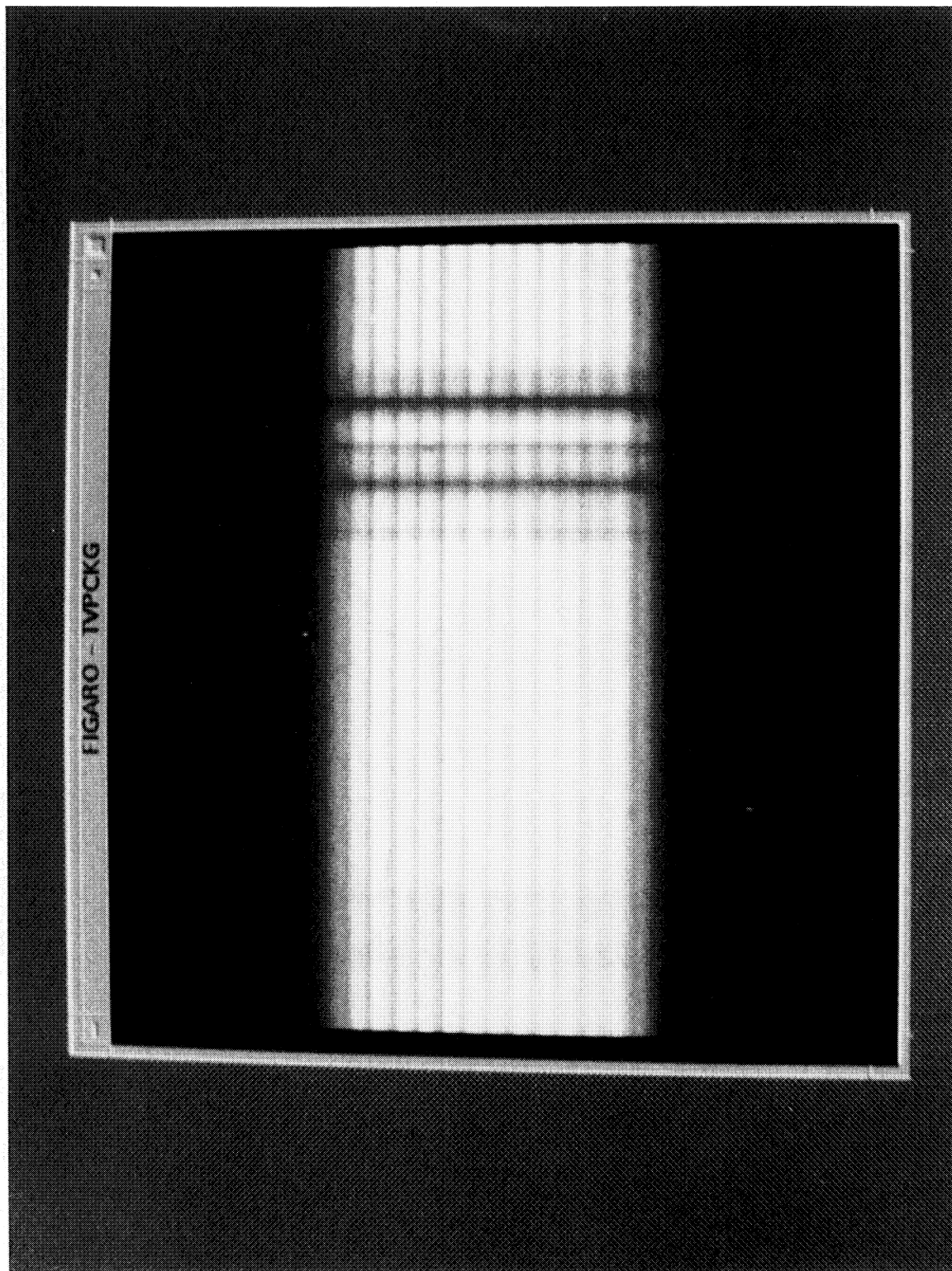
Figure 3. CCD image showing a 1000-s integration on ϵ Ori at the Na D_1 line (5895.924 Å), obtained on 1994 January 20 with the (masked) 35-CIS. Wavelength increases to the right; the spectral coverage is 2.54 Å. 14 CIS slices may be counted in the spatial direction. Note that hyperfine splitting (separation 21.2 mÅ, or 1.08 km s^{-1}) is clearly visible in two of the interstellar D_1 velocity components present towards this star.
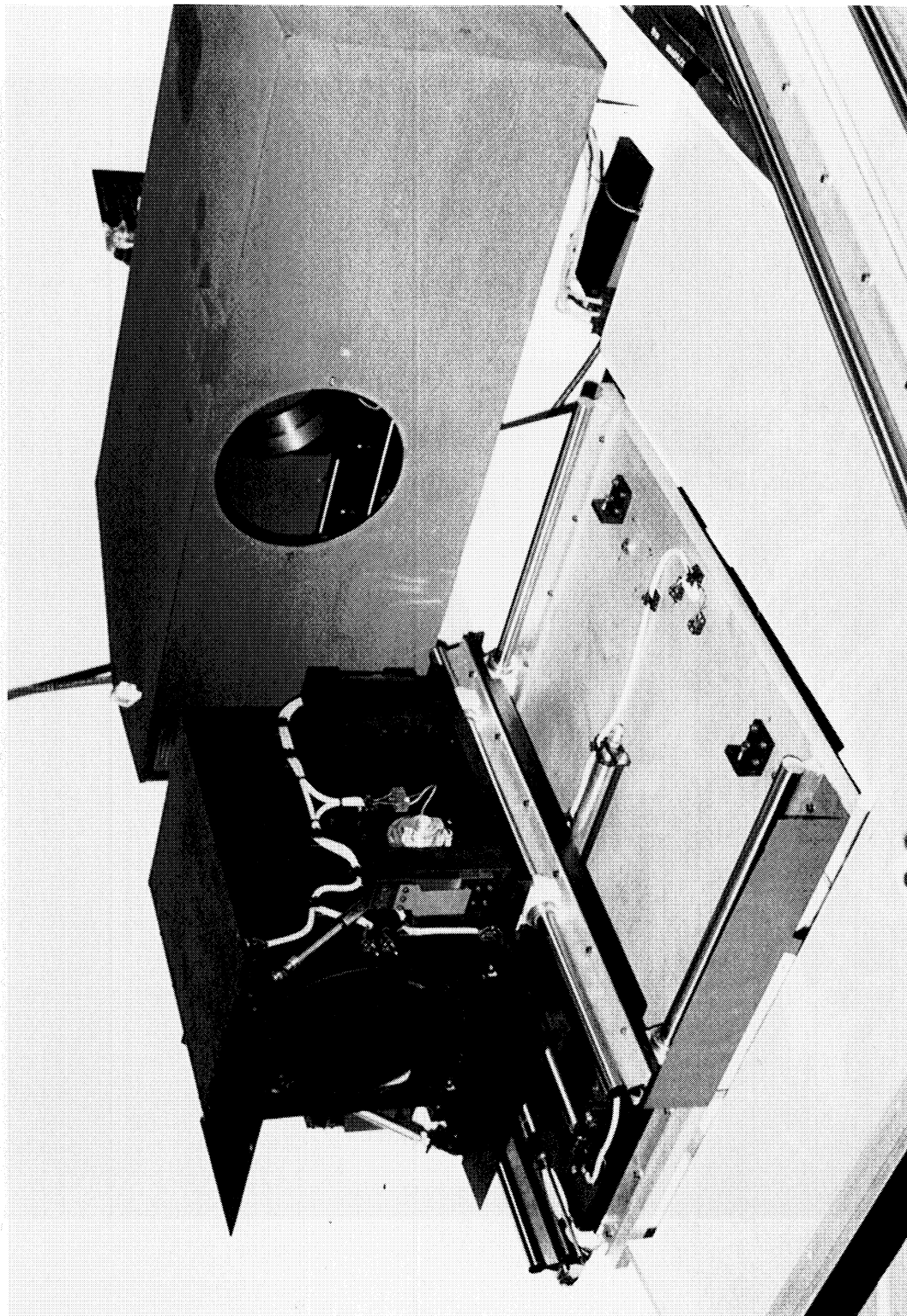
Figure 4. The UHRF echelle-collimator unit appears on the left, out of the optical axis, which runs to the centre of the UCLES collimator mirror inside the box on the right. Note the rails used to shift the unit on to the optical axis, and those used to allow for focusing. Note also the Hartmann shutters on the front of the unit, between which the collimator lens can be seen. Compare this photograph with Figs 5 and 6.
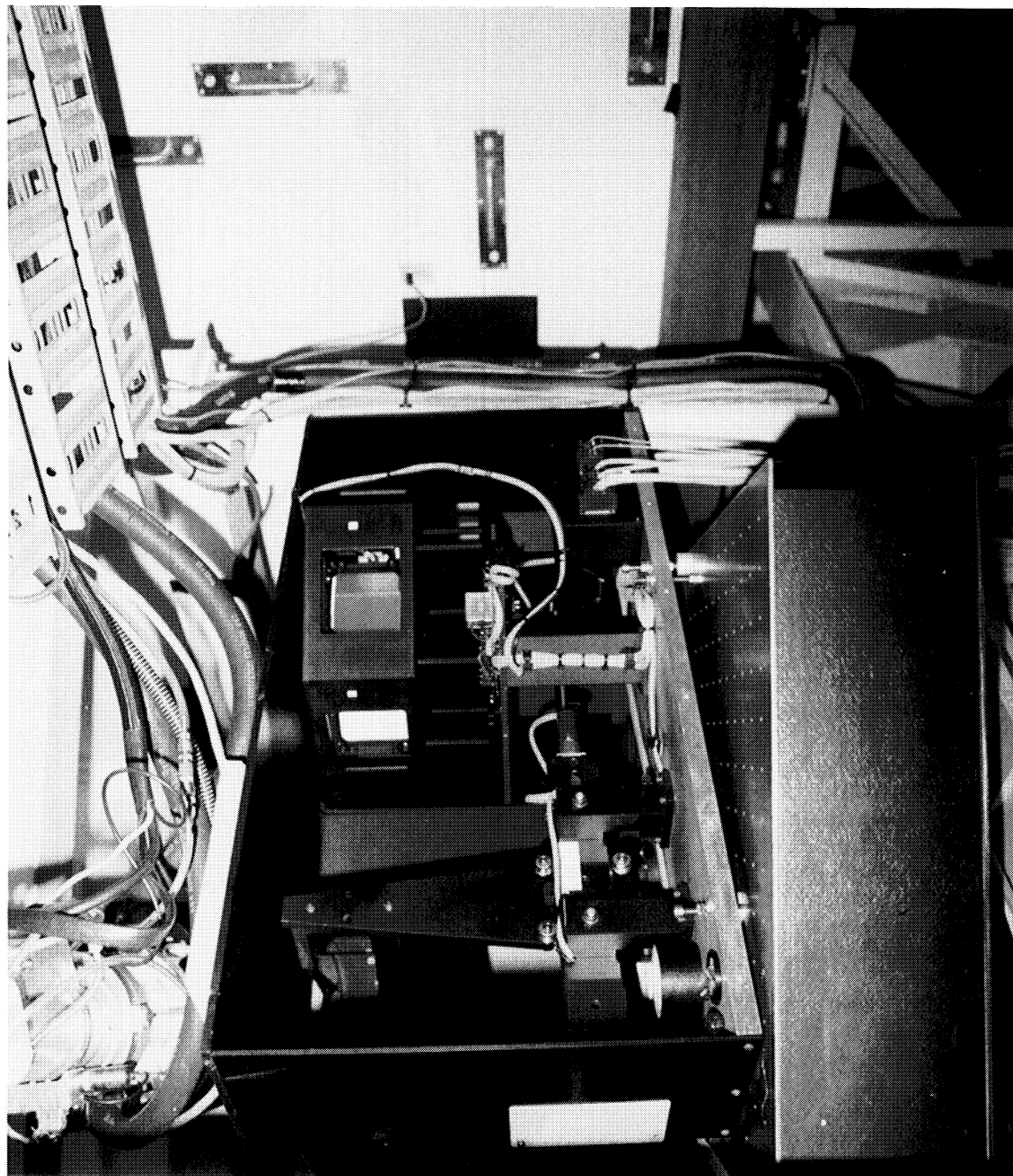
Figure 8. The UHRF cross-disperser unit, shown without its side plate in order to reveal the secondary collimator mechanism on the left and the grating turret at the centre. The entire unit has been mounted at 2° inclination on the optical table used to support the UCLES prism system. The slit-area facilities are behind the false wall on the right.

an accuracy and repeatability better than 5 arcsec, equivalent to a few CCD pixels on the focal plane. The echelle-collimator unit also contains motorized Hartmann shutters, which are necessary for accurate focusing at each selected spectral region. The entire assembly can be moved in front of the UCLES collimator to intercept the beam.

4.3 Cross-disperser unit

The echelle orders are spread-out by a choice of four 110 mm square cross-disperser gratings (blazed for the *U*, *B*, *V* and *R* spectral regions, with 2400, 1800, 1200 and 1200 g mm^{-1}, respectively), mounted on a carousel mechanism which also includes two flat mirrors coated for blue and red wavelengths [Figs 7 and 8 (opposite p. 326)]. These mirrors are intended for use in combination with narrow-band filters to isolate echelle orders as an alternative to the gratings. The filters can be placed in either of the two filter wheels available in the post-slit (slicer) area of UCLES-UHRF.

A single actuator moves a six-way tangent arm mechanism, which rotates all the cross-disperser gratings (and the two mirrors) to bring selected echelle orders to the centre of the field. The accuracy and repeatability are the same as for the echelle grating tilt. Each grating has been mounted with an angular offset to compensate for its particular blaze angle.

A diverging lens placed before the carousel recollimates the beam coming from the echelle-collimator unit. This 'secondary' collimator is not achromatic, and it also has to be displaced along the optical axis by a linear actuator. Its position is measured to the nearest 100 μm (although this is not very critical, as the main focusing is done with the primary collimator using Hartmann shutters). After the carousel, a fixed aspheric lens projects the spectrum on the detector. The introduction of a secondary collimated beam of reduced
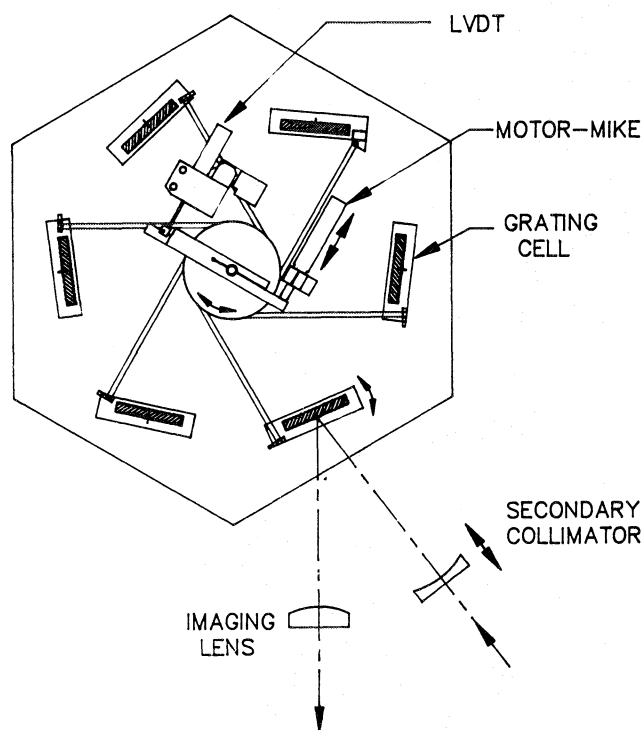

Figure 7. The turret containing the cross-disperser gratings.

diameter simplified the solution to the cross-disperser problem, allowing the use of smaller gratings.

The cross-disperser unit sits on the same optical table which supports the UCLES prisms, and its presence does not affect the operation of UCLES.

4.4 Lower resolution modes

In addition to the nominal one million mode, UHRF has been provided with a choice of two focal reducer lenses (item L in Fig. 1) to increase spectral coverage and energy per pixel at lower resolutions. The lenses are highly aspheric, and the nominal resolving powers are 3×10^5 and 6×10^5; however, the measured instrumental profiles (Section 7.1) actually indicated somewhat higher resolving powers. The use of these lenses displaces the focal plane, so the detector is mounted on a motorized carriage travelling along a precision rail.

4.5 Detector carriage

This is a strong frame able to carry either the IPCS or a cryostat with a CCD. It also has provision to mount the cylindrical lens (when in use, see Section 7.3), and a fast shutter protects the detector from accidental over-illumination. A large box with a small rectangular aperture is used as a light baffle to reduce stray light.

5 CONTROL

The control system for UHRF at the hardware level is a fully integrated extension to the existing UCLES modular control system (discussed in detail by Fish 1988). The provision of a UHRF-type facility was anticipated during the design of UCLES. Due to the complexity of the optical systems (of both UCLES and UHRF), a high level of automation under computer control was regarded as essential. The control philosophy that was adopted aims to insulate the observer from individual functions. This approach leads to efficient use of telescope time, and will eventually lend itself to remote observing.

The UHRF-specific hardware consists of a number of standard UCLES control modules assembled into two UCLES-style control racks, linked to the existing control bus and using the existing Local Instrument Microcomputer (LIM) and software. The only change required in the LIM software is the addition of UHRF control functions to an ASCII text file.

In both UCLES and UHRF, the requirements of large optical components needing to be positioned accurately and repeatably are satisfied by providing absolute encoding and DC servo-control. Importantly, the components themselves, rather than the motors that drive them, are encoded. Absolute encoding makes it possible to power down the control system between mode changes, without losing the calibration. Following UCLES philosophy, all encoders are Linear Variable Displacement Transducers (LVDT).

In order to provide all the possible options to the observer, and present them in a friendly, easy-to-use manner, all the software running on the Observatory Instrumentation Computer (OIC) is being written within the ADAM environment (STARLINK Project).
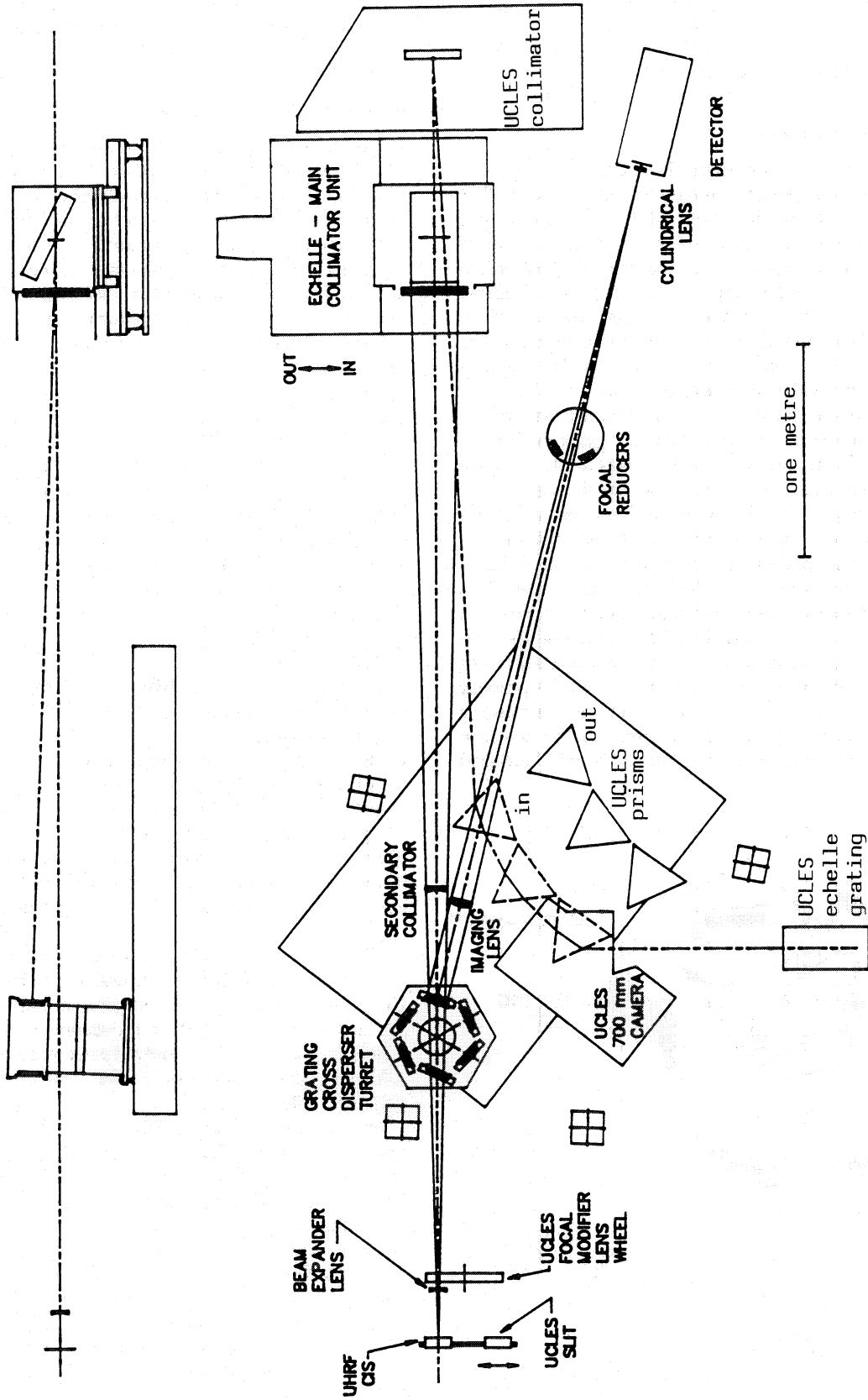
Figure 9. The optical layout of the AAT east coudé room, showing the locations of the optical components of both UCLES and UHRF.

1995MNRAS.272..323D

6 OPERATION

Fig. 9 is a simplified layout of the east coudé room at the AAT, containing UCLES and UHRF.

Configuration of all this equipment for UHRF operation involves the following remotely controlled actions:

(1) replace UCLES slit by UHRF Confocal Image Slicer;
(2) place the beam expander lens on axis;
(3) place the collimator-echelle unit on axis, and
(4) withdraw UCLES prisms and place them in their UV position.

6.1 Wavelength positioning

Since there are about 140 echelle orders with lengths ranging from 200 mm in the UV to 800 mm in the IR, accurate positioning of the target wavelength at the centre of a detector window of only 20 or 30 mm is a difficult task.

In its final form, it is intended that only the desired wavelength will have to be specified in order to configure the UHRF, the appropriate parameters then being calculated and written to a control file. An OIC-based program contains fundamental information from the ray-tracing model developed for the optical design. This model is being upgraded with positions of many target wavelengths observed during commissioning phases after the final alignment of the entire instrument. The control program will read control files and will use the information to perform all necessary calculations to send target values to the LIM, which in turn will supervise the mode change and will return status to the OIC.

At the time of writing, this mode of operation has not been fully implemented, but more than a dozen spectral regions of special interest have been located by requesting encoder values from the LIM to find echelle orders one by one and identifying known lines in the Th-Ar spectrum. The stability of the encoding system allows any instrumental configuration to be repeated in the future to bring a particular wavelength to the same position within a few pixels. This mode of operation is described in the preliminary UHRF User's Manual (Spyromilio 1994).

6.2 Focusing

To achieve maximum spectral resolution, the position of the collimator-echelle unit has to be within 50 μm of the target value. This is done by using the Hartmann shutters and cross-correlating images of the Th-Ar calibration lamp. The first approximation is done by using the positions of primary and secondary collimators predicted by the computer model. Then only one Hartmann cycle is usually necessary to verify the fine positioning done by the motor-mike mechanism shown in Fig. 5.

6.3 Acquisition and guiding

The aperture of the CIS-35 is located at about 60 mm from the optical axis, so the telescope pointing has to be offset accordingly.

The image of this aperture illuminated by a seeing disc is clearly visible on the TV screen, and the AAT autoguider system produces very good results. The field of view is

typically adjusted to be less than 1 arcmin, and this is good enough for both acquisition and guiding, given the excellent pointing of the AAT. It must be noted that atmospheric dispersion may offset the selected wavelength outside the 1.5 × 1.5 arcsec square aperture on the TV guider, particularly for observations in the blue, so it is very important to reposition the image using the AAT routines for atmospheric dispersion compensation, just before a new frame is exposed.

6.4 Detectors

The UHRF was originally conceived to work with an IPCS which can deliver 10-μm pixels and relatively large detective areas. During the commissioning phases it was found more convenient to use the AAO's Thomson CCD, which has 1024 × 1024 pixels of 19 μm each. The higher quantum efficiency of the Tektronix CCD also makes this detector attractive, particularly for fainter objects, although the larger (24-μm) pixels mean that the instrumental resolution will only just be properly sampled.

We also note that the BIGMIC detector being developed at UCL (Fordham et al. 1994) may prove to be a particularly appropriate detector for the UHRF. This detector will be free from both cosmic ray events and CCD read-out noise, and will provide both a larger detective area (61 × 46 mm²) and much smaller (10-μm) pixels. The latter will be particularly useful if oversampling of the UHRF instrumental profile is required. It is hoped that BIGMIC may be tested on the instrument in the near future.

7 PERFORMANCE

Spectra obtained during the commissioning of the UHRF clearly indicate that the instrument has met its design specifications, and astrophysical results have been published separately in this Journal (Barlow et al. 1995; Crawford et al. 1994a,b). This section concentrates on the resolution, throughput and stray light performances.

7.1 Instrumental profile and spectral resolution

As the UHRF resolves the lines emitted by the Th-Ar calibration lamp (which cannot therefore be used to evaluate the instrumental profile), a frequency-stabilized He-Ne laser, which provides an unresolved line at 6328.160 Å, was used to determine the instrumental profile. The laser was used to illuminate a very narrow (10-μm) slit, and the projected image was sampled by the rather coarse pixels (19 μm) of a Thomson CCD. The FWHM of a Gaussian fit to the line profile indicates a resolving power of 993 000 (2.40 pixel; Fig. 10).

Fig. 11 shows one of the first UHRF spectra, obtained using the same 10-μm slit. The spectrum is of the interstellar Na D_2 line towards ζ Oph, and the hyperfine splitting (separation 1.01 km s⁻¹) is clearly resolved in several of the discrete velocity components (especially that with a heliocentric velocity of −9 km s⁻¹). To our knowledge, this is the highest resolution optical astronomical spectrum ever obtained.

Subsequent tests with the CIS-35 image slicer (which produces a 30-μm wide slit) have yielded an instrumental FWHM as low as 0.303 ± 0.007 km s⁻¹ ($R = 990\,000$,

measured in 1993 August). Thus use of the image slicer has in no way impaired the resolution. In order to check the resolution at a wavelength other than that of the red He-Ne laser, a stabilized green (5433.647 Å) He-Ne laser was borrowed from the Australian CSIRO National Measurement Laboratory. This also yielded an instrumental FWHM of 0.303 (±0.005) km s^{-1} (2.28 pixel), demonstrating that, as expected, the UHRF resolution is independent of wavelength.

For the lower resolution modes, preliminary tests with the stabilized red He-Ne laser indicate that the resolving powers are 450 000 and 750 000, respectively.

7.2 Throughput

Fig. 12 shows one of the few spectra obtained under photometric conditions during the commissioning runs. The UHRF has resolved the very sharp blue wing of the Na I D$_2$ line towards κ Vel and at the same time, using the CIS-35, achieved 50 000 counts (e$^-$) per bin above background in the continuum of this $V=2.50$ star in only 600 s with the Thomson CCD. Assuming ×8 binning, and a read-out noise of 3.9 electrons per binned pixel (AAO Observer's Guide), these numbers indicate that a S/N ratio of 30 could be attained in 2.5 h on a $V=9.0$ star, which means that the brightest stars in the Large Magellanic Cloud are potentially observable. The limiting magnitude would be fainter if a photon-counting detector (e.g. BIGMIC, see Section 6.4) were to be employed.

7.3 Stray light

All spectrographs are prone to light scattering off the various optical components and surfaces (see, e.g., Cardelli, Ebbets & Savage 1990 for the case of the GHRS echelle spectrograph). In the case of echelle spectrographs, this is usually corrected by subtracting the light background measured in the interorder region. Unfortunately, in the case of the UHRF the cylindrical lens originally used to collapse the slicer output on to the detector (Section 4.1) made it impossible to measure this interorder background directly: light from the interorder region was funnelled on to the centre of the detector together with light from the order under observation. As a consequence, determination of the amount of scattered light and correction for it became the main outstanding problems in calibrating UHRF spectra.

Experiments have shown that most of the background light is due to scattered red light from the source, and that this can be reduced significantly by careful baffling and the use of appropriate filters. Nevertheless, the problem of evaluating the remaining scattered light remained.

In the end it was decided to remove the cylindrical lens altogether, and mask the length of the CIS-35 output slit down to about 8 mm (an example is shown in Fig. 3). This

Figure 10. The UHRF instrumental response function, determined by means of a stabilized He-Ne laser for a 10-μm entrance slit obtained in 1992 July. The velocity scale is relative to the He λ6328.160 line. A Gaussian fit gives a FWHM of 0.302±0.003 km s^{-1} ($R=9.93\times10^5$).
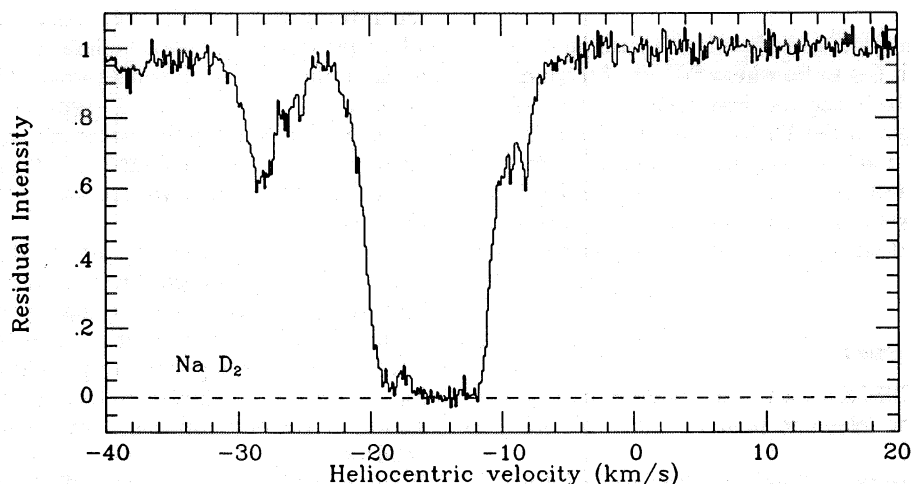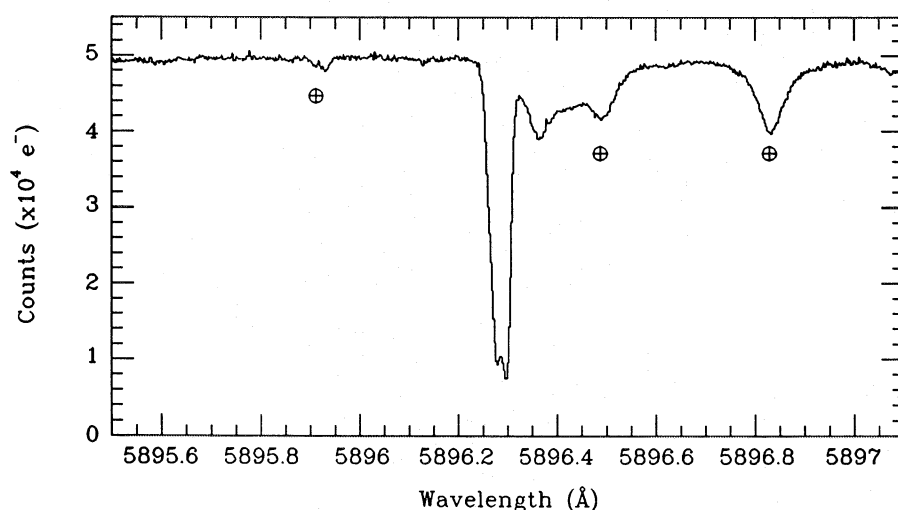

Figure 11. The interstellar Na D$_2$ line observed towards ζ Oph with a 10-μm entrance slit in 1992 July. Note the clear resolution of the hyperfine structure (separation 1.01 km s^{-1}) in the -9 km s^{-1} velocity component.

Figure 12. The interstellar Na D_1 line towards κ Vel ($V = 2.50$), obtained with the CIS-35 during photometric conditions in 1993 May. The exposure time was 600 s. Note the clear resolution of the hyperfine structure in the core of the line. Atmospheric absorption features are labelled as such.

allowed part of the interorder region to fall on the detector, enabling the proper determination of the background light level, but it has, of course, resulted in lower overall through-put. It is hoped that this will only be an interim measure; further experiments are in hand, with the aim of producing an image slicer able to deliver shorter slits without the need for masking.

8 DATA REDUCTION

In order to facilitate data reduction, the detector is mounted in such a way that its pixel rows follow the direction of the image of the slit. Any small angular difference is measured by cross-correlating the profiles extracted from the ends of the image of a comparison Th-Ar line, and then the entire detector has to be rotated using a precision micrometer available at the mounting flange. The image of the slit is precisely horizontal. On-chip binning by a factor of 4, or even 8, along the spatial direction is an effective way to reduce read-out noise without having a detrimental effect due to accumulated cosmic rays which, in any case, limit individual exposure times to less than ~ 1800 s.

Wavelength calibration is achieved by means of a Th-Ar lamp. Owing to the small wavelength coverage of the detec-tor (1–3 Å, depending on the wavelength), some important spectral regions were found to be lacking in strong, pre-viously identified, Th-Ar lines. However, it was discovered that, by removing the Th-Ar lamp from its usual position in the UCLES pre-slit calibration unit and placing it directly in front of the image slicer aperture, the number of detectable lines was increased sufficiently to permit accurate wave-length calibration in all spectral regions explored to date. Results from ray-tracing models had indicated extremely linear dispersion. This situation was confirmed in all the observed spectral regions, where the residuals from linear fits were less than 0.001 Å.

As UHRF works in single echelle order mode, data extraction is quite straightforward, and may be accomplished

with any data reduction package designed to cope with two-dimensional echelle images, for example FIGARO (Shortridge 1988) or ECHOMOP (Mills & Webb 1989).

9 CONCLUSIONS

The combination of UHRF with the CIS-35 is a unique facility providing the highest spectral resolution for inter-stellar and stellar work for relatively faint stars. The instru-ment has achieved its common-user status and is available to the community. A preliminary User's Manual has been produced by the AAO (Spyromilio 1994).

Improvements are still under way. These include fully automated operation similar to UCLES, the implementation of an anamorphic CIS, and the possible use of BIGMIC as a detector. These will further strengthen the capabilities of what is already a unique instrument.

assembly of electronic control racks. The mechanical components were produced by the workshop of the Department of Physics and Astronomy, UCL. Once again, the excellent working atmosphere, motivation and professionalism of the AAO staff were a great help to the success of the UHRF commissioning. The UHRF was mainly funded by SERC grant GR/F/23880, with some complementary funding from the AAO.

REFERENCES

Barlow M. J., 1984, Proposal to the AAO Board: 'The potential importance for interstellar absorption-line studies of the proposed AAT coudé echelle spectrograph'

Barlow M. J., Silk J., 1977, ApJ, 211, L83

Barlow M. J., Crawford I. A., Diego F., Dryburgh M., Fish A. C., Howarth I. D., Spyromilio J., Walker D. D., 1995, MNRAS, 272, 333 (this issue)

Butcher H. R., 1971, Proc. Astron. Soc. Aust., 2, 21

Cardelli J. A., Ebbets D. C., Savage B. D., 1990, ApJ, 365, 789

Crawford I. A., Rees P. C. T., Diego F., 1987, Observatory, 107, 147

Crawford I. A., Barlow M. J., Diego F., Spyromilio J., 1994a, MNRAS, 266, 903

Crawford I. A., Spyromilio J., Barlow M. J., Diego F., Lagrange A. M., 1994b, MNRAS, 266, L65

Diego F., 1988a, in Robinson L. B., ed., Instrumentation for Ground-Based Astronomy, Proc. Ninth Santa Cruz Summer Workshop in Astronomy and Astrophysics. Springer Verlag, p. 6

Diego F., 1988b, PhD thesis, Univ. London

Diego F., 1993, Appl. Opt., 32, 6284

Diego F., Walker D. D., 1985, MNRAS, 217, 347

Diego F., Charalambous A., Fish A., Walker D., 1990, Proc. SPIE 1235. Int. Soc. Opt. Eng., Bellingham, p. 562

Elitzur M., Watson W. D., 1978, ApJ, 222, L141

Enard D., 1982, in Crawford D. L., ed., Proc. SPIE 331. Int. Soc. Opt. Eng., Bellingham, p. 232

Fish A. C., 1988, in Robinson L. B., ed., Instrumentation for Ground-Based Astronomy, Proc. Ninth Santa Cruz Summer Workshop in Astronomy and Astrophysics. Springer Verlag, p. 628

Fordham J. L. A., Bone D. A., Michel-Murillo R., Norton T. J., Butler I. G., Airey R. W., 1994, in Proc. SPIE 2198, Instrumentation in Astronomy VIII. Int. Soc. Opt. Eng., Bellingham, p. 829

Gillingham P. R., 1988, in Robinson L. B., ed., Instrumentation for Ground-Based Optical Astronomy; Present and Future. Springer-Verlag, New York, p. 134

Hirst C. J., Walker D. D., Diego F., Fish A. C., Charalambous A. C., 1986, in Crawford D. L., ed., Proc. SPIE 627. Int. Soc. Opt. Eng., Bellingham, p. 721

Hobbs L. M., 1969, ApJ, 157, 135

Hunten D. M., 1974, in Marton L., ed., Methods of Experimental Physics, Vol. 12A, Academic Press, p. 193

Lambert D. L., Sheffer Y., Crane P., 1990, ApJ, 359, L19

Meyer D. M., Hawkins I., Wright E. L., 1993, ApJ, 409, L61

Mills D., Webb J., 1989, Gemini, 26, 10

Pettini M., 1988, Proc. Astron. Soc. Aust., 7, 527

Richardson E. H., Fletcher J. M., Grundman W. A., 1984, in Ulrich M., Kjär K., eds, Proc. IAU Colloq. 79, Very Large Telescopes, Their Instrumentation and Programs. ESO, Garching, p. 469

Shortridge K., 1988, Starlink User Note No. 86

Simmons J. E., Drake R. M., Hepburn L. V., 1982, in Crawford D. L., ed., Proc. SPIE 331. Int. Soc. Opt. Eng., Bellingham, p. 427

Spyromilio J., 1994, Ultra-High-Resolution Facility Operating Manual, Anglo-Australian Observatory

Tull R., 1972, in Lausten S., Reiz A., eds, Auxiliary Instrumentation for Large Telescopes. ESO/CERN, Geneva, p. 259

Walker D. D., Diego F., 1985, MNRAS, 217, 355

Walker D. D., Diego F., Charalambous A., Hirst C. J., Fish A. C., 1986, Proc. SPIE 627. Int. Soc. Opt. Eng., Bellingham, p. 291